Acta Neurochirurgica (2019) 161:2505–2511
https://doi.org/10.1007/s00701-019-04099-6

ORIGINAL ARTICLE - BRAIN TUMORS

Correlations between the trigeminal nerve microstructural changes and the trigeminal-pontine angle features

Huize Pang[1] · Hao Sun[2] · Guoguang Fan[1]

Received: 7 August 2019 / Accepted: 7 October 2019 / Published online: 6 November 2019

Abstract

Background Morphological and microstructural changes of the trigeminal nerve due to neurovascular compression (NVC) have been reported in primary trigeminal neuralgia (PTN) patients. This investigation was to examine the relationship between the trigeminal-pontine angle and nerve microstructural changes.

Methods Twenty-five patients underwent microvascular decompression (MVD) for trigeminal neuralgia, and 25 age- and sex-matched controls were studied. The two groups underwent high-resolution three-dimensional MRI and diffusion tensor imaging (DTI). Bilateral trigeminal-pontine angle, cross-sectional area of cerebellopontine angle (CPA) cistern, and the length of trigeminal nerve were evaluated. The mean values of fractional anisotropy and apparent diffusion coefficient at the site of NVC were also measured. Correlation analyses were performed for the trigeminal-pontine angle and the diffusion metrics (FA and ADC) in PTN patients.

Results The mean trigeminal-pontine angle and FA value on the affected side was significantly smaller than the unaffected side and the control group ($p < 0.001$), while the mean ADC value was significantly increased ($p < 0.01$). When taking the conflicting vessel types into consideration, the angle affected by the superior cerebellar artery (SCA) was statistically sharper than when affected by other vessels ($p < 0.01$). However, there were no significant changes in the area of the CPA cistern or the length of the trigeminal nerve between the groups. Correlation analyses showed that the trigeminal-pontine angle was positively correlated with FA and negatively correlated with ADC.

Conclusions A sharp trigeminal-pontine angle may increase the chance of NVC and exacerbate nerve degeneration, which may be one of the supplementary factors that contribute to the pathogenesis of trigeminal neuralgia.

Keywords Primary trigeminal neuralgia · 3D-FIESTA · DTI · Trigeminal-pontine angle

Introduction

Trigeminal neuralgia (TN) is a debilitating facial pain syndrome with a prevalence of 1–2 per 10,000 individuals [18]. It is characterized by provocable pain that recurs in one or more branches of the trigeminal nerve distribution [15]. The pain can be triggered by mild sensory stimulation and can disrupt daily living. Neurovascular compression (NVC) is a widely accepted mechanism of TN. The leading hypothesis for its etiology is long-term NVC causing focal nerve axonal and myelin abnormities, following ectopic generation of impulses and ephaptic transmissions between the surrounding injured axons. However, the absence of neurovascular conflict is encountered in up to 10% of patients with primary trigeminal neuralgia (PTN) symptoms [26]. High-resolution magnetic resonance imaging (MRI), especially three-dimensional fast-imaging employing steady-state acquisition (3D-FIESTA) imaging, is implemented to visualize the relationship between the trigeminal nerve and surrounding blood vessels while it makes simultaneous morphological measurements [2, 21, 28, 29]. It has been suggested that a small

This article is part of the Topical Collection on *Brain Tumors*

✉ Guoguang Fan
fanguog@sina.com

Huize Pang
ophelia0702@163.com

Hao Sun
ivy_071602@126.com

[1] Department of Radiology, The First Hospital of China Medical University, Shenyang, Liaoning Province, China

[2] Department of Clinical Epidemiology, The First Hospital of China Medical University, Shenyang, Liaoning Province, China

cerebellopontine angle (CPA) cistern, a sharp trigeminal-pontine angle, and the length of the cistern segment of the trigeminal nerve are diagnostic markers for PTN patients [8, 10]. The trigeminal nerve root forms an angle with the site where it emerges from the pons, which has been suggested to be a potential point of compression on the nerve. Recent advances in MRI technology have enabled more investigations into the microstructural changes of the trigeminal nerve. Diffusion tensor imaging (DTI) qualifies the amount of non-random water molecule diffusion dynamics and potentially enables probing of the microanatomy of neural tissues in vivo. The DTI metric fractional anisotropy (FA) can provide insight into the integrity of trigeminal nerve fibers. Most experts suggest that DTI can enable identification of axonal atrophy and demyelination of trigeminal nerve root caused by NVC [4, 5, 17, 20]. Despite these findings, there are still no investigations into the correlation between the trigeminal-pontine angle and nerve pathological changes. Thus, we conducted this pilot investigation to identify morphological and microstructural changes of the trigeminal nerve contributing to the pathogenesis of trigeminal neuralgia and correlate the diffusion metrics with the trigeminal-pontine angle.

Methods and materials

Participants

This study was conducted between November 2017 and May 2019. We recruited 25 PTN patients with unilateral NVC (11 men, 14 women; age range 30–75 years, mean age 52.75 ± 10.1 years). The average symptom duration was 20 months, and the diagnosis of all TN patients was confirmed in accordance with the diagnostic criteria of typical TN [1] and was treated with microvascular decompression (MVD). To validate the study, 25 sex- and age-matched healthy participants (12 men, 13 women, age range 40–70 years, and a mean age of 55.2 ± 10.2 years) were also recruited in the study as healthy control (HC). The HC had no history of facial pain. Patients with secondary TN, bilateral symptoms, or those with metal implants were excluded. Written informed consent was obtained from each participant before entering the study, and the study was approved by the institutional ethics committee of our hospital.

Magnetic resonance imaging

All participants were imaged with a 3.0-T MRI scanner (Signa HDx, GE Healthcare, Milwaukee, WI, USA) using 3D-FIESTA and DTI. An eight-channel head coil was used with foam padding and braces to restrict head motion. All the acquired images were aligned to the anterior commissure-posterior commissure (AC-PC) plane. The following imaging protocols were used: (a) 3D-FIESTA sequence with repetition time/echo time (TR/TE) = 5.0 ms/1.9 ms, flip angle = 60°, the field of view = 200 mm × 170 mm, matrix = 320 × 288, and slice thickness = 0.6 mm without gap and two acquisitions; (b) DTI with a single-shot spin echo and echo-planar imaging protocol, TR/TE = 7100 ms/94 ms, field of view = 200 mm × 170 mm, matrix = 160 × 160, $b = 1000$ s/mm^2 with diffusion gradients applied in 30 diffusion directions, and slices of 2.0 mm without gap.

Data processing

3D-FIESTA images were transferred to a post-processing workstation (Advantage Workstation, ADW 4.4, GE Medical Systems). All patients' images were observed in axial, coronal, and sagittal planes to evaluate the relationship between the nerve and surrounding structures. The morphology was measured using the following methodology. The trigeminal-pontine angle was measured between the medial margin of the trigeminal nerve and the anterior surface of the pons at the root entry zone (REZ). The location of REZ was defined as the first 3-mm segment of the trigeminal nerve as it exits the pons [19]. The CPA cistern is a subarachnoid space filled with cerebrospinal fluid; it was defined as the area between the anterior surface of the pons and cerebellum and the posterior surface of the arachnoid membrane that rested on the petrous bone, including the REZ of trigeminal nerve. The cerebellar flocculus was considered the posterior limit, and the basilar artery in the pre-pontine cistern as the anterior limit. When the basilar artery was distorted, midline was defined as the anterior limit. The length of the cistern segment of the trigeminal nerve was measured in the same axial images from the REZ to Meckel's cave. It was defined as the distance from the point where the nerve emerged from the pons to the narrow aperture of Meckel's cave (Fig. 1).

The original DTI data were processed with Functool software in the AW4.4 workstation (GE Medical Systems, Milwaukee, WI, USA) to generate fractional anisotropy (FA) and an apparent diffusion coefficient (ADC). In the patient group, ROIs were placed over the NVC of the trigeminal nerve (Figs. 2 and 3). The diagnostic criteria of NVC were defined as no visible cerebrospinal fluid between the nerve and its adjacent arteries at the symptomatic side on 3D-FIESTA MRI. The site of ROI is located in the center of the nerve, and the surrounding cerebrospinal fluid components are avoided as much as possible. The ROI area is as consistent as possible, approximately 20 ± 7.5mm^2. For the HC, ROIs were placed over the site of NVC in the corresponding TN patient group. All the morphological parameters and diffusion metrics were measured independently by two observers who were blinded to the purpose of this study and to which side of the patient's face was symptomatic. The mean values from the two observers were utilized for analysis.

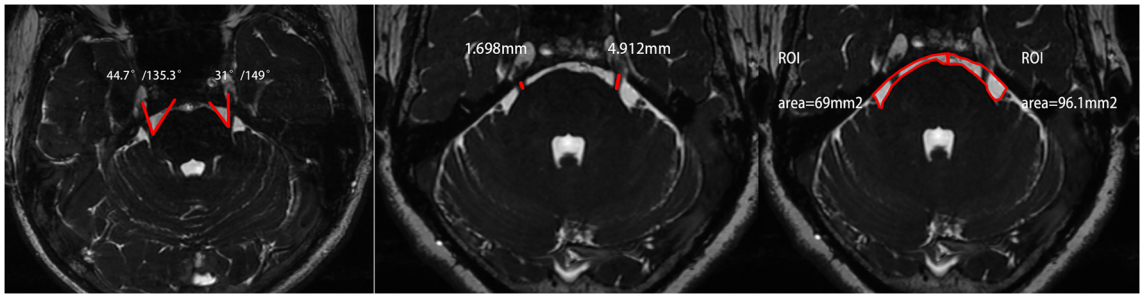

Fig. 1 Axial three-dimensional fast-imaging employing steady-state acquisition (3D-FIESTA) MRI showing delineation of the angle between the trigeminal nerve and anterior surface of the pons (**a**), measurement of the length of the cistern segment of the trigeminal nerve (**b**), and measurement of the cross-sectional area of cerebellopontine angle cistern (**c**)

Statistical analysis

All analyses were performed with SPSS 23 software (SPSS Inc, Chicago, IL, USA). Results are expressed as the median (interquartile ranges) (minimum, maximum) for non-normally distributed variables. The trigeminal-pontine angle, the cross-sectional area of CPA cistern, the length of the cistern segment of the trigeminal nerve, and the values of FA and ADC were compared between the affected and unaffected side and healthy controls by Kruskal-Wallis followed by pairwise comparisons among the three groups. Also, the trigeminal-pontine angles were compared according to the conflicting vessel types between superior cerebellar artery (SCA) and other vessels using Mann-Whitney *U* test. A $p \leq 0.05$ was considered statistically significant. Spearman correlation analyses were used to compare trigeminal-pontine angle and diffusion metrics.

Results

Table 1 summarizes the morphological parameters and diffusion metrics.

Comparison of morphological parameters

The trigeminal-pontine angle on the affected side was significantly less than the unaffected side ($p < 0.001$) and HC ($p = 0.005$, Fig. 4). However, there was no difference in the cross-sectional area of the CPA cistern and the length of the cistern segment of the trigeminal nerve between the affected and unaffected side and HC ($p = 0.874$ and $p = 0.900$, respectively).

Comparison of diffusion metrics

The mean value of FA at the site of NVC was significantly attenuated, and the mean value of ADC was significantly increased compared with the unaffected side (FA $p = 0.006$, ADC $p = 0.015$) and HC (FA $p < 0.001$, Fig. 5 and ADC $p = 0.014$, Fig. 6).

Correlation between trigeminal-pontine angle and diffusion metrics

Correlation analyses revealed that the trigeminal-pontine angle was significantly and positively correlated with the FA ($r = 0.513$, $p < 0.01$, Fig. 7) and negatively correlated with the ADC ($r = -0.548$, $p < 0.01$, Fig. 8).

Role of conflicting vessel types

The main responding vessel in sixteen patients was the superior cerebellar artery (SCA), in four patients was the anterior inferior cerebellar artery(AICA), in three patients was the vertebral artery(VA), in one patient was the posterior inferior

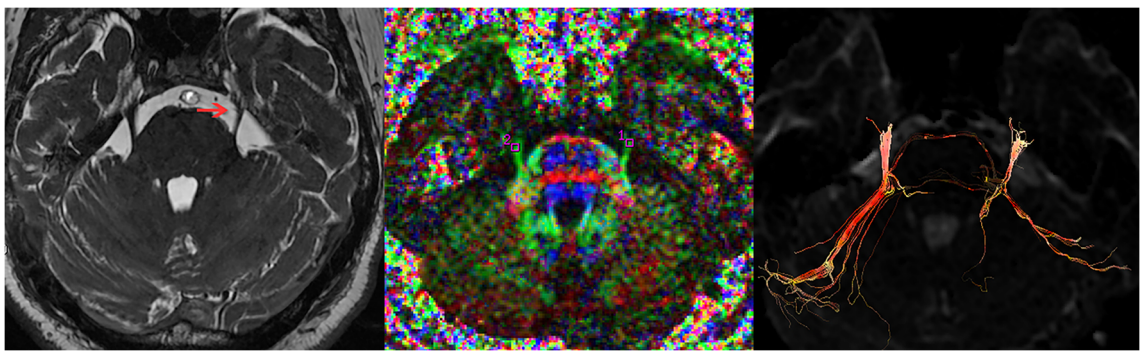

Fig. 2 A 56-year-old male TN patient, suffering left maxillofacial pain for more than 2 years. **a** 3D-FIESTA MRI shows bypass of SCA (arrow) across the cistern segment of the trigeminal nerve. **b** Regions of interest (ROIs) were manually drawn on the cistern segment of the trigeminal nerve on color-coded diffusion tensor index maps. **c** Trigeminal nerve fiber bundles show the left nerve fiber is finer than the right side

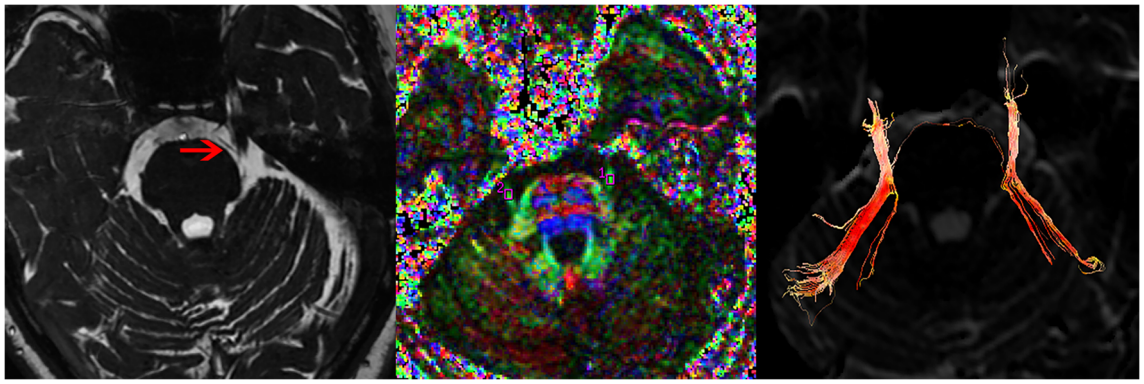

Fig. 3 A 59-year-old female TN patient, suffering left maxillofacial pain for more than 1 year. **a** 3D-FIESTA MRI shows span of SCA (arrow) near the root entry zone (REZ) of the trigeminal nerve. **b** ROIs were manually drawn on the REZ of the trigeminal nerve on color-coded diffusion tensor index maps. **c** Trigeminal nerve fiber bundles show the left nerve fiber is finer than the right side

cerebellar artery (PICA), and in one was the multiple vascular contact (AICA and PICA). Patients with a SCA conflict had a significantly smaller trigeminal-pontine angle than non-SCA patients (p = 0.004, Mann-Whitney U test). Table 2 summarizes the trigeminal-pontine angle according to the conflicting vessel type.

Discussion

TN is a recurrent pain syndrome caused by a variety of mechanisms, but NVC is considered one of the primary causes [9, 24]. Besides, TN is also considered related to various morphological and microstructural changes. Thus, this study explored the morphological and microstructural changes of trigeminal nerve in PTN patients. Moreover, we correlated the trigeminal-pontine angle with the nerve microstructural changes. To our knowledge, such a hypothesis has not been verified yet using MRI techniques.

In our study, the trigeminal-pontine angle on the affected side was significantly smaller than the unaffected side and the HC. When taking the conflicting vessel types into consideration, the trigeminal-pontine angle of SCA is statistically smaller than that of other vessels. Anatomically, the trigeminal nerve originates from the anterolateral side of the brainstem and, after exiting the brainstem, it travels forward and down, where it enters the Meckel's cave below the free edge of the tentorium and forms the trigeminal ganglion. Previous studies suggest that nerve fibers in the ipsilateral trigeminal nerve root of TN patients trend toward spatial distribution, rather than keeping a fixed position. Some scholars found a tendency for the distribution of medial nerve fibers to be concentrated, while the lateral nerve fibers show electrophysiological abnormalities [14, 27]. Also, Gudmundsson et al. [7] found that the differences in trigeminal trunk angles would impact the spatial arrangement of branches of nerve fibers within the nerve roots. They believed that the differences in trigeminal root fiber distribution and branching might be related to trigeminal trunk angles, but they did not explain the specific relationship

Table 1 Comparisons of morphological and microstructural parameters in primary trigeminal neuralgia patients and healthy control (HC)

Variables	Affected side	Unaffected side	HC	p value (affected side vs. unaffected side vs. HC)	p value (affected side vs. unaffected side)	p value (affected side vs. HC)
Trigeminal-pontine angle (°)	38.60 (35.85, 43.55) (27.20, 50.10)	48.00 (44.30, 53.25) (38.30, 64.10)	46.45 (41.13, 48.68) (32.40, 59.80)	< 0.001	< 0.001	0.005
Length of cistern segment of nerve (mm)	7.64 (6.55, 9.95) (4.10, 13.10)	7.90 (6.55, 10.00) (3.49, 14.50)	7.95 (7.10, 8.43) (4.95,9.45)	0.900	-	-
Area of CPA (mm^2)	171.80 (124.45, 241.65) (64.50, 320)	173.60 (132.90, 223.80) (68.70, 291)	178.60 (151.98, 191.25) (118.05, 238.50)	0.874	-	-
FA	0.35 (0.32, 0.36) (0.22, 0.41)	0.39 (0.34, 0.41) (0.25, 0.56)	0.39 (0.38, 0.42) (0.35, 0.44)	< 0.001	0.006	< 0.001
ADC ($\times 10^{-9}$ mm^2/s)	1.96 (1.82, 2.10) (1.70, 2.21)	1.83 (1.74, 1.91) (1.38, 2.07)	1.83 (1.73, 1.93) (1.61, 2.17)	0.005	0.015	0.014

Data are presented as median (interquartile ranges) (minimum, maximum) for non-normally distributed variables

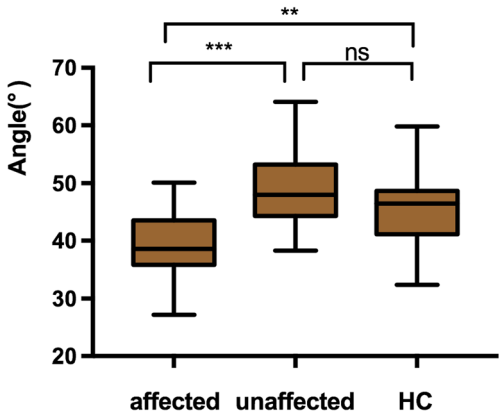

Fig. 4 Box and whisker plots of trigeminal-pontine angle between affected, unaffected side, and healthy control (HC). Graph showing that the trigeminal-pontine angle on the affected side was significantly smaller than that of the unaffected side and healthy control (HC). There was no statistical difference between the unaffected side and healthy control. (*p < 0.05, **p < 0.01, ***p < 0.001) ns = not significant

between trigeminal trunk angle and the pathogenesis of TN. Furthermore, Ha et al. [8] found that the trigeminal-pontine angle on the affected side in PTN patients is significantly reduced. It is inferred that the sharp trigeminal-pontine angle may increase the probability of neurovascular contact, which in turn leads to the occurrence of TN symptoms. Leal et al. found that the most common cause of trigeminal neuralgia with NVC grades II and III was in greater proportion at REZ by the vascular loop, which is usually the SCA [13]. After descending from the basilar artery, the elongated SCA forms a vascular loop, which could contact or oppress the superomedial part of the nerve root. In addition, Sindou et al. [25] also found that the most common location of trigeminal NVC was superomedial to the nerve root. The common location of trigeminal NVC may be attributed to the high proportion of the conflict of SCA. When the trigeminal-

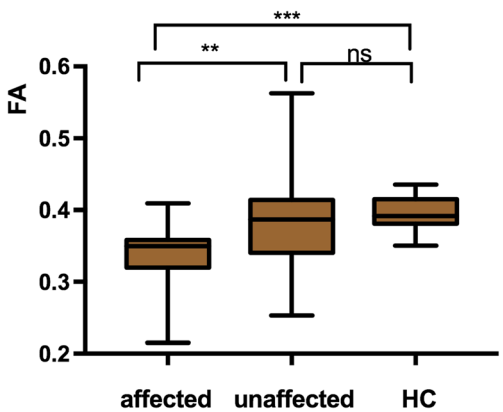

Fig. 5 Box and whisker plots of fractional anisotropy (FA) between affected, unaffected side, and HC. Graph showing that the value of fractional anisotropy (FA) on the affected side was significantly smaller than that of the unaffected side and healthy control (HC). There was no statistical difference between the unaffected side and healthy control. (*p < 0.05, **p < 0.01, ***p < 0.001) ns = not significant

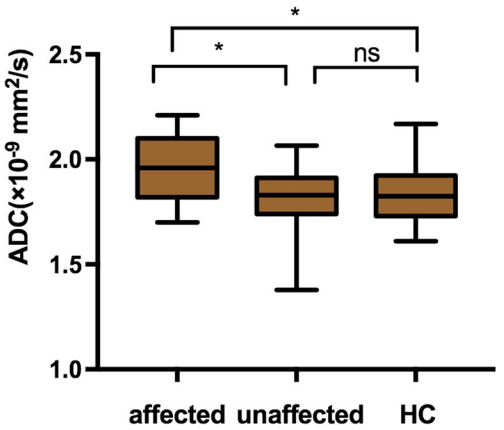

Fig. 6 Box and whisker plots of apparent diffusion coefficient (ADC) between affected, unaffected side, and HC. Graph showing that the value of apparent diffusion coefficient (ADC) on the affected side of trigeminal neuralgia patients was larger than that of the unaffected side and healthy control (HC). There was no statistical difference between the unaffected side and healthy control. (*p < 0.05, **p < 0.01, ***p < 0.001) ns = not significant

pontine angle is small, the distance between the medial aspect of the nerve root and the vascular loop of the SCA is minimal. A small trigeminal-pontine angle may influence the genesis of neurovascular conflict in the medial side of the trigeminal nerve. Also, nerve fibers on the inner side of the nerve are concentrated with the functional fibers. In accordance with the "short-circuit theory" [11], there were conduction short circuits between those functional nerve fibers, thus causing a repeated "trigger point"–like pain syndrome. This could explain our hypothesis that a small trigeminal-pontine angle may increase the chance of NVC on the medial side of the trigeminal nerve, which is supported by our results. Thus, a small trigeminal-pontine angle may be considered as a risk factor for NVC in PTN patients.

In addition, we found that the mean FA value is significantly decreased, and the mean ADC value is significantly increased at the site of NVC in TN patients when compared with the unaffected side and controls using DTI. DTI is a non-

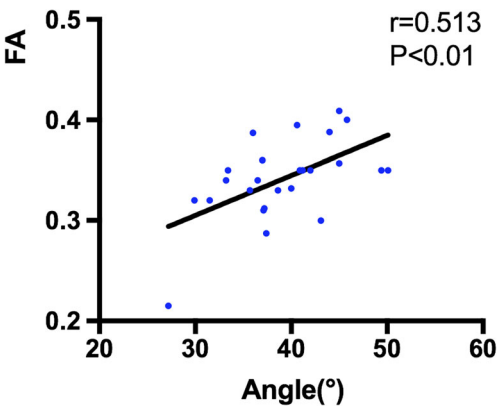

Fig. 7 Correlation analyses between trigeminal-pontine angle and FA value

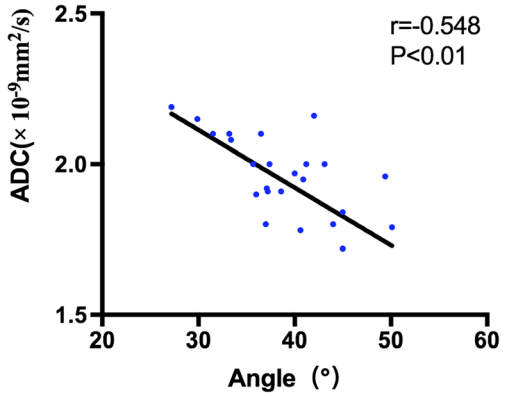

Fig. 8. Correlation analyses between trigeminal-pontine angle and ADC value

invasive MRI technique that allows in vivo visualization of white matter tracts. Leal et al. [12] found that the value of FA on the affected side was significantly reduced in PTN patients, the value of the ADC was increased, and the reduced FA was negatively correlated with the increased ADC using DTI. From a biological perspective, the FA provides insight into white matter integrity and direction, and the decrease of the FA value is due to demyelination or axonal degeneration of the nerve fibers caused by vascular compression, mostly via the SCA. The ADC value reflects the diffusion of water molecules in the tissue, and thus, long-term vascular compression would cause chronic hypoperfusion of the nerve root and accelerated water molecule diffusion, thus increasing the ADC value [3, 6, 16].

Simultaneously, the correlation analyses suggest that the smaller the trigeminal-pontine angle, the more substantial the microstructural changes of the nerve root. The change in dynamic structural factors causes secondary microstructural heterogeneity, playing a role in TN mechanisms and causing the manifestation of symptoms. However, the coefficient is not relatively strong, possibly because the trigeminal-pontine angle could facilitate TN by increasing the chance of neurovascular conflict, in an indirect way to cause demyelination and axonal degeneration.

In the present investigation, there were no significant changes in the length of the cistern segment of the nerve on the affected side. However, Park et al. and Praise et al. [22, 23] found that the length of the cistern segment of the trigeminal nerve on the affected side was significantly shorter than the length on the unaffected side. This may be due to relatively small sample size; the difference of the length of the cistern segment of the trigeminal nerve may be underestimated. The cross-sectional area of the CPA cistern on the affected side did not appear to be significantly different between TN patients and the HC. Conversely, Kawano et al. and Praise et al. [10, 22] found that the area of the CPA cistern on the affected side was significantly reduced in PTN patients. This may be attributed to the small sample size and presence of senile encephalatrophy in the elderly, which may make the area larger when compared to younger patients.

Limitations of the present investigation include its relatively small sample size and lack of a long-term follow-up of patients to evaluate the prognosis value of morphological parameters and diffusion metrics. DTI also have several technical limitations. The partial volume effect specifically caused by the small size of the root that is bathed in cerebrospinal fluid may confound DTI measurements. Besides, involuntary patient movement and magnetic susceptibility effects may affect the image quality and measurement. In addition, the manual delineation of the trigeminal nerve and ROI placement may be prone to inter-rater variability. Thus, the value of the trigeminal-pontine angle as a diagnostic marker may be overestimated, and an automated measurement and larger sample size in future studies may solve these problems.

Table 2 Comparison of trigeminal-pontine angle according to the conflicting vessel types in primary trigeminal neuralgia patients

Vessel types	Number	Trigeminal-pontine angle (°)
SCA	16 (64%)	37.05 (33.25, 40.45) (27.20,45.00)
Non-SCA	9 (36%)	43.10 (39.90, 47.60) (36.00,50.10)
Z	-	− 2.775
p value	-	0.004

Data are presented as median (interquartile ranges) (minimum, maximum) for non-normally distributed variables

Conclusion

The trigeminal-pontine angle on the affected side was significantly smaller than the unaffected side and HC. The FA value was significantly decreased, and the ADC value was significantly increased. When taking vessel types into consideration, the trigeminal-pontine angle affected by the SCA is significantly sharper than that impacted by other vessels. Further, the trigeminal-pontine angle was positively correlated with FA and negatively correlated with ADC. This investigation suggests that a sharp trigeminal-pontine angle might increase the chance of neurovascular conflict and the degree of trigeminal nerve demyelination and may be a possible exacerbating factor for TN.

Compliance with ethical standards

Conflict of interest The authors declare that they have no conflict of interest.

Ethical approval All procedures performed in studies involving human participants were in accordance with the ethical standards of the institutional and/or national research committee and with the 1964 Helsinki Declaration and its later amendments or comparable ethical standards.

Informed consent Informed consent was obtained from all individual participants included in the study.

Abbreviations ADC, apparent diffusion coefficient; AICA, anterior inferior cerebellar artery; CPA, cerebellopontine angle; DTI, diffusion tensor imaging; FA, fractional anisotropy; HC, healthy control; MVD, microvascular decompression; NVC, neurovascular compression; PICA, posterior inferior cerebellar artery; PTN, primary trigeminal neuralgia; REZ, root entry zone; ROI, region of interest; SCA, superior cerebellar artery; VA, vertebral artery; 3D-FIESTA, three-dimensional fast-imaging employing steady-state acquisition

References

1. Arnold M (2018) Headache classification committee of the international headache society (IHS). The international classification of headache disorders, 3rd edition. Cephalalgia 38(1):1–211
2. Benes L, Shiratori K, Gurschi M, Sure U, Tirakotai W, Krischek B, Bertalanffy H (2005) Is preoperative high-resolution magnetic resonance imaging accurate in predicting neurovascular compression in patients with trigeminal neuralgia? Neurosurg Rev 28(2):131–136
3. Bihan DL (1995) Molecular diffusion, tissue microdynamics and microstructure. [J]. NMR Biomed 8(7):375–386
4. Chen ST, Yang JT, Yeh MY, Weng HH, Chen CF, Tsai YH (2016) Using diffusion tensor imaging to evaluate microstructural changes and outcomes after radiofrequency rhizotomy of trigeminal nerves in patients with trigeminal neuralgia. PLoS One 11(12):e0167584
5. Desouza DD, Hodaie M, Davis KD (2013) Abnormal trigeminal nerve microstructure and brain white matter in idiopathic trigeminal neuralgia. Pain 155(1):37–44
6. Desouza DD, Hodaie M, Davis KD (2016) Structural magnetic resonance imaging can identify trigeminal system abnormalities in classical trigeminal neuralgia. Front Neuroanat 95 eColletion
7. Gudmundsson K, Rhoton AL Jr, Rushton JG (1971) Detailed anatomy of the intracranial portion of the trigeminal nerve. J Neurosurg 35(5):592–600
8. Ha SM, Kim SH, Yoo EH, Han IB, Shin DA, Cho KG, Chung SS, Park YS (2012) Patients with idiopathic trigeminal neuralgia have a sharper-than-normal trigeminal-pontine angle and trigeminal nerve atrophy. Acta Neurochir 154(9):1627–1633
9. Jannetta PJ, Mclaughlin MR, Casey KF (2005) Technique of microvascular decompression. Technical note. Neurosurg Focus 18(5):E5
10. Kawano Y, Maehara T, Ohno K (2014) Validation and evaluation of the volumetric measurement of cerebellopontine angle cistern as a prognostic factor of microvascular decompression for primary trigeminal neuralgia. Acta Neurochir 156(6):1173–1179
11. Kerr FW, Miller RH (1966) The pathology of trigeminal neuralgia: electron microscopic studies. Arch Neurol *15*(3):308–319
12. Leal PRL, Roch JA, Hermier M, Souza MA, Cristino-Filho G, Sindou M (2011) Structural abnormalities of the trigeminal root revealed by diffusion tensor imaging in patients with trigeminal neuralgia caused by neurovascular compression: a prospective, double-blind, controlled study. Pain 152(10):2357–2364
13. Leal PR, Barbier C, Hermier M, Souza MA, Cristino-Filho G, Sindou M (2014) Atrophy changes in the trigeminal nerves of patients with trigeminal neuralgia due to neurovascular compression and their association with the severity of compression and clinical outcomes. J Neurosurg 120(6):1484–1495
14. Ley A, Montserrat L, Bacci F, Ley A Jr (1975) Clinical and electrophysiological studies on sensory conduction mediated by the accessory rootlets of the human trigeminal nerve. J Neurosurg 42(5):513–521
15. Love S, Coakham HB (2001) Trigeminal neuralgia: pathology and pathogenesis. Brain 124(Pt 12):2347–2360
16. Lutz J, Linn J, Mehrkens JH, Thon N, Stahl R, Seelos K, Bruckmann H, Holtmannspotter M (2010) Trigeminal neuralgia due to neurovascular compression: high-spatial-resolution diffusion-tensor imaging reveals microstructural neural changes. Radiology 258(2):524–530
17. Lutz J, Thon N, Stahl R, Lummel N, Tonn JC, Linn J, Mehrkens JH (2016) Microstructural alterations in trigeminal neuralgia determined by diffusion tensor imaging are independent of symptom duration, severity, and type of neurovascular conflict. J Neurosurg 124(3):823–830
18. Manzoni GC, Torelli P (2005) Epidemiology of typical and atypical craniofacial neuralgia. [J]. Neurol Sci 26(2):s65–s67
19. Mistry AM, Niesner KJ, Lake WB, Forbes JA, Shannon CN, Kasl RA, Konrad PE, Neimat JS (2016) Neurovascular compression at the root entry zone correlates with trigeminal neuralgia and early microvascular decompression outcome. World Neurosurg 95:208–213
20. Neetu S, Sunil K, Ashish A, Jayantee K, Usha KM (2015) Microstructural abnormalities of the trigeminal nerve by diffusion-tensor imaging in trigeminal neuralgia without neurovascular compression. Neuroradiol J 29(1):13–18
21. Ni S, Su W, Li X, Zeng Q, Liu Y, Zhu S, Wu C (2009) Enhanced three-dimensional fast spoiled gradient recalled MRI combined with magnetic resonance angiography for preoperative assessment of patients with trigeminal neuralgia. J Clin Neurosci 16(12):1555–1559
22. Parise M, Acioly MA, Ribeiro CT, Vincent M, Gasparetto EL (2013) The role of the cerebellopontine angle cistern area and trigeminal nerve length in the pathogenesis of trigeminal neuralgia: a prospective case-control study. Acta Neurochir (Wien) 155(5):863–868
23. Park SH, Hwang SK, Lee SH, Park J, Hwang JH, Hamm IS (2009) Nerve atrophy and a small cerebellopontine angle cistern in patients with trigeminal neuralgia. J Neurosurg 110(4):677–637
24. Qu CC, Zeng SQ, Zhang JQ, Wang ZG (2009) A single-blinded pilot study assessing neurovascular contact by using high-resolution MR imaging in patients with trigeminal neuralgia. Eur J Radiol 69(3):459–463
25. Sindou M, Howeidy T, Acevedo G (2002) Anatomical observations during microvascular decompression for idiopathic trigeminal neuralgia (with correlations between topography of pain and site of the neurovascular conflict). Prospective study in a series of 579 patients. Acta Neurochir (Wien) 144(1):1–12
26. Sindou M, Leston J, Howeidy T, Decullier E, Chapuis F (2006) Micro-vascular decompression for primary trigeminal neuralgia (typical or atypical). Long-term effectiveness on pain; prospective study with survival analysis in a consecutive series of 362 patients. Acta Neurochir (Wien) 148(12):1235–1245
27. Stechison MT, Møller A, Lovely TJ (1996) Intraoperative mapping of the trigeminal nerve root: technique and application in the surgical management of facial pain. Neurosurgery 38(1):76–81
28. Tarnaris A, Renowden S, Coakham HB (2007) A comparison of magnetic resonance angiography and constructive interference in steady state-three-dimensional fourier transformation magnetic resonance imaging in patients with hemifacial spasm. Br J Neurosurg 21(4):375–381
29. Zhou Q, Liu Z, Li C, Qu C, Ni S, Zeng Q (2011) Preoperative evaluation of neurovascular relationship by using contrast-enhanced and unenhanced 3D time-of-flight MR angiography in patients with trigeminal neuralgia. Acta Radiol 52(8):894–898